JOURNAL OF THE KOREAN ASTRONOMICAL SOCIETY
36: 49 ~ 54, 2003

HII REGIONS IN THE SPIRAL GALAXY NGC 3389

HAMED ABDEL-HAMID[1,2], SANG-GAK LEE[1], AND PETER NOTNI[3]
[1] Astronomy Program, SEES, Seoul National University, Seoul 151-742, Korea
[2] National Research Institute of Astronomy and Geophysics, Cairo, Egypt
[3] Astrophysikalisches Institut Potsdam, D-14482 Potsdam, Germany
e-mail: hamed@astro.snu.ac.kr, sanggak@astrosp.snu.ac.kr, pnotni@aip.de
(Received June 9, 2003; Accepted June 23, 2003)

ABSTRACT

CCD observations in V, I and H_α for NGC 3389 are used to present photometry of 61 HII regions. Their positions, diameters and absolute luminosities have been determined. The luminosity and size distribution functions of the HII regions in NGC 3389 are discussed.

Key words : galaxies: spiral-HII regions—galaxies: individual (NGC 3389)

I. Introduction

NGC 3389 is a spiral galaxy, classified by de Vaucouleurs et al. (1991) as an SA galaxy and by Sandage & Tammann (1981) as an Sc galaxy. NGC 3389 is one of Leo triplet with galaxies, NGC 3384 and NGC 3379. The lack of detailed photometric studies for NGC 3389 and its normal undistorted morphology in spite of a group of galaxies, motivate us to do photometry for NGC 3389 and study its stellar population properties. The basic parameters of NGC 3389 are given in Table 1.

HII regions in galaxies are powered by the newly formed stars, therefore they give clues for the recent star formation in galaxies. The total H_α luminosity can be used to quantify their current star formation rate. Therefore we concern firstly with the investigation of the HII region properties of NGC 3389: their luminosity and size distributions.

This is the first CCD work on the HII regions of NGC 3389. Hodge & Kennicutt (1983) presented the off-set positions for 50 identified HII regions in NGC 3389 in their photographic surveys of the HII regions in galaxies, and Kennicutt & Kent (1983) gave the total integrated H_α flux and luminosity for the galaxy.

II. Observations and data reduction

V, I and H_α CCD observations of NGC 3389 were carried out using 1.23 m telescope of Calar Alto observatory on 5-6 February 1995 with Tek CCD which have 1024 × 1024 pixels and a plate scale of $0.502''$ pixel^{-1}. Observations were done with seeing varying from $0.7''$ to $1.2''$ during the night. Four frames of H_α image were taken with H_α interference filter whose central bandpass is 6580 Å with a FWHM of 100 Å. Four frames in V filter and three frames in I filter were observed. Table 2 gives the log of observations. All data reductions were done using the image processing program MIDAS. The standard image processing routine has been done, then all frames were carefully aligned using the position of the common foreground stars in the frames. The sky backgrounds were measured using MIDAS task FIT/FLATSKY with area offset from the galaxy in the margin of frame. After sky subtraction, the cosmic ray effects are removed by median filter. A weighted mean image for each filter was computed. In order to get an accurate continuum level we have choosen two continuum bands on either side of H_α; V and I are used. The fluxes of the selected stars in the three bands (I, V and H_α) were used to determine the H_α continuum level. Then the H_α image was corrected for the continuum contribution. For flux calibration, we compare the integrated measurements within an aperture whose diameter equal to three arcminutes, which contains the entire visible disk of NGC 3389 to a limiting surface brightness of 25 mag/arcsec^2 with the total absolute luminosity given by Bell & Kennicutt (2001). This total integration normalized by the total absolute luminosity quoted by Bell & Kennicutt (2001), for the same diameter size ($3'$), to get the observed measurements in units of erg s^{-1}. The absolute flux has been measured with the same specification of central wavelength and bandwidth (λ 6580/100 Å) as that of ours. Bell & Kennicutt (2001) used the distance of 24 Mpc (Shanks 1997) to convert the fluxes to luminosity.

III. HII regions identification

Fig. 1 shows the continuum-subtarcted Hα image of NGC 3389. A visiual identification of the HII regions was firstly done, by displaying the continuum-subtarcted Hα image with different scaling factors and the boundaries were measured at the discernable level. To measure the contour dimensions of each HII region (dx and dy) a graphical interface precedure within MIDAS was used. However if the HII regions are crowded or lie in a diffuse bright background the largest closed

Corresponding Author: H. Abdel-Hamid

Table 1. Basic Parameters for NGC 3389

R.A. (2000.0)	$10^{h}\ 48^{m}\ 28^{s}$	
Dec (2000.0)	$12^{d}\ 31^{'}\ 59^{''}$	
Type	SA(s)	de Vaucouleurs et al. 1991
Diameters	2.8×1.3 arcminutes	
radial Velocity	1306±6 km/sec	de Vaucouleurs et al. 1991
M_B	-19.82	Tully 1988
Lα	1.08×10^{41}erg/sec	D=24 Mpc, Bell & Kennicutt 2001
Lα aperture size	3 arc minutes	

Table 2. Log of the Observations

Filter	V	I	H_α
Exposure Time in seconds	100, 500, 500, 600	500, 500, 500	1000, 1000, 1000, 1500
Date	February 5-6, 1995		
Observer	P. Notni		

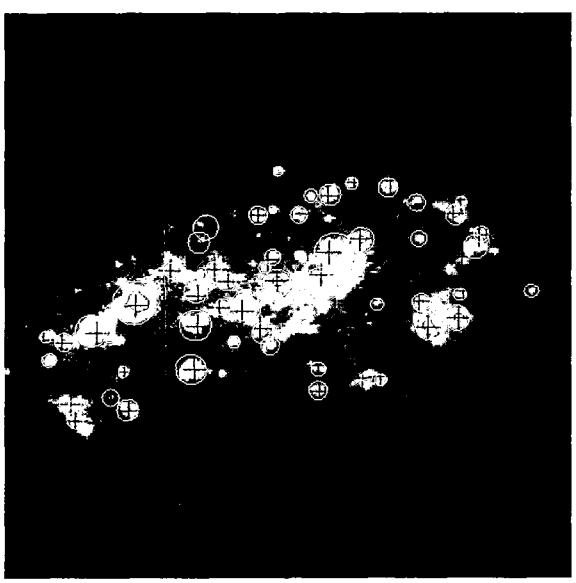

Fig. 1.— Continuum subtracted H_α image for NGC 3389 with HII regions of this study (ellipses) and those of Hodge& Kennicutt (1983) (crosses).

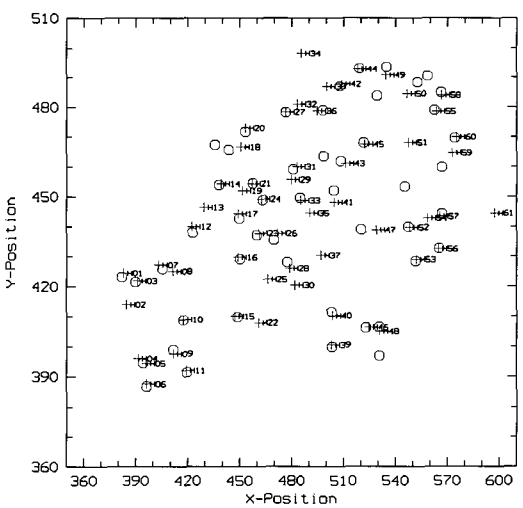

Fig. 2.— Identification of 61 HII regions of this study (open circles) in comparison with those of Hodge & Kennicutt (1983) (crosses).

contour is used to measure the HII region boundary. From these methods we fixed dimensions of the HII regions. In some cases it was needed to justifity the aperture radius by hand. The aperture radius used for the flux integration was calculated as follows:

$$r = (\sqrt{dx^2 + dy^2})/2 \qquad (1)$$

The aperture radius used to estimate the backgroud flux in the proximity of each HII region is varied according to how much HII regions are crowded.

Figs. 1 and 2 illustrate the positions of 61 HII regions in NGC 3389 in comparison with those of Hodge & Kennicutt (1983); Hodge provided the off-set positions of HII regions from the center of NGC 3389 and a map of NGC 3389 by private communication. We find a good agreement between our position measurments and their position data for 40 objects. The rest ten HII regions of Hodge & Kennicutt (1983) have no counterparts in our data. These ten HII regions may lie below our identification criterion, their off-set positions and identification names are given in Table 3. Twenty one HII regions are newly identified.

The integrated flux and the background flux for each HII region are measured, then the flux corrected for the background to give the net flux. The main source of error in the net fluxes are due to either the incorrect estimation of the background or the inaccurate estimate of the boundaries, or both. To estimate the uncertainties in the flux measurements multiple trials have been done to measure the flux of individual HII regions. We found statistically that the uncertainities in the measured fluxes vary from less than 10% for the isolated regions to 20% for the crowded regions.

The measured H_α fluxes are corrected for Galactic extinction, $A(0.65\mu m) = 0.073$ mag (Schlegel et al. 1998). To remove the contamination by the [NII] emission lines in the measured H_α fluxes, the total fluxes were multiplied by a factor of 0.75 according to Kennicutt (1983); the factor gave the average ratio of $H_\alpha/(H_\alpha+[NII])$ in the spirals. They have used the same filter (100 $\AA$ bandwidth at 6580 $\AA$) in their measurments for galaxies with radial velocities under 3000 km s^{-1}. Sixty one HII regions were identified, and the equatorial coordinates of their positions, diameters in parsec, the logarithmic lumnosities and the corresponding Hodge & Kennicutt (1983) identifications (HK-ID) are listed in Table 4.

Table 3. Un-identified Hodge & Kennicutt (1983) HII regions

KH-ID	X-off	Y-off
10	031	010
12	027	009
25	-001	007
32	-012	-006
36	-017	017
37	-017	-028
40	-025	001
43	-029	019
44	-032	020
47	-036	004

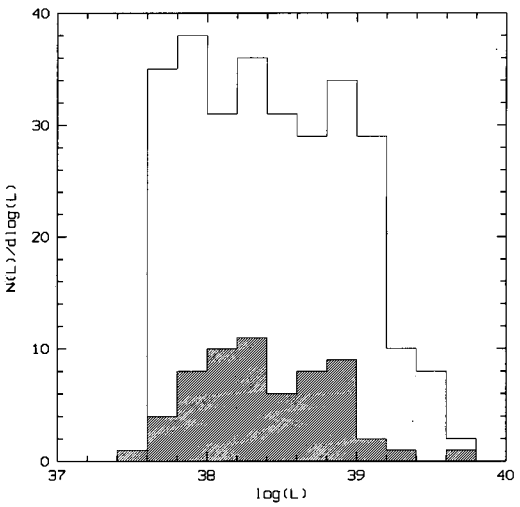

Fig. 3.— The LF of HII regions for NGC 3389 (hatched histogram) against that for NGC 6384 (solid line).

IV. The Luminosity Function

The H_α luminosity of the HII regions in NGC 3389 spans a range $L(H_\alpha) \approx 3\times10^{37} - 6\times10^{39}$ erg s^{-1}. This range of $L(H_\alpha)$ luminosity is frequent in Sa-Sb galaxies (see for example in Thilker et al. 2002). The HII regions with $L(H_\alpha)$ luminosity higher than 10^{39} erg s^{-1} are found in late-type (Sc-Irr) normal galaxies or in interacting galaxies (Kennicutt et al. 1989). The luminosites of the 61 HII regions are binned in logarithmic interval of 0.2 dex and ploted in Fig. 3.

In Fig. 3, our LF is compared with that of Feinstein (1997) for Sb spiral galaxy NGC 6384. The HII regions in both galaxies exhibit nearly the same $L(H_\alpha)$ range, but the number of the HII regions of NGC 6384 is about four times larger than that of NGC 3389. The reason for that is the absolute blue luminosity of NGC 6384 (M_B=-21.31) is approximately four times that of NGC 3389. A mimic relation is founded on NGC 6822 by Hodge et al. (1989).

In order to fit the luminosity distribution of the HII regions independantly of the LF bin size, the cumulative luminosity distribution have been done following Feinstein (1997). The cumulative LF is presented in Fig. 4 in comparison with that of NGC 6384 (Feinstein 1997), LFs for two galaxies normalized by their number of the HII regions at log(L) of 38.6. The LFs are in agreement at the luminosities log(L) $\leq$ 39.0, while they are incongruent at higher luminosities log(L) $>$ 39.0. This is due to NGC 6384 has 49 HII regions with luminosities higher than 39.0 (log) while NGC 3389 contains only 4 HII regions. The two galaxies have different absolute blue luminosities as well as different spiral types. This result may confirm that NGC 3389 is neither Sc spiral nor an interacting galaxy.

Table 4. HII region in NGC 3389

Name	R.A.(2000.0)	Dec. (2000.0)	Diameter (pc)	log L (erg/sec)	HK-ID
H01	$10^h48^m28.80^s$	$12^d31'49.67''$	277	38.24	1
H02	10 48 28.96	12 31 44.43	370	38.29	-
H03	10 48 28.58	12 31 48.38	472	38.74	2
H04	10 48 29.11	12 31 35.33	264	38.11	-
H05	10 48 28.99	12 31 34.54	293	37.90	3
H06	10 48 29.12	12 31 31.18	442	38.61	4
H07	10 48 28.08	12 31 51.04	815	38.97	5
H08	10 48 27.85	12 31 49.95	328	37.98	-
H09	10 48 28.41	12 31 36.13	440	37.69	6
H10	10 48 27.98	12 31 41.84	279	38.03	7
H11	10 48 28.27	12 31 33.34	555	38.78	8
H12	10 48 27.18	12 31 57.46	1138	39.80	9
H13	10 48 26.82	12 32 00.72	302	37.88	-
H14	10 48 26.33	12 32 04.66	421	38.38	11
H15	10 48 26.98	12 31 42.42	798	38.96	13
H16	10 48 26.52	12 31 52.30	799	38.82	14
H17	10 48 26.20	12 31 59.63	591	38.41	15
H18	10 48 25.70	12 32 10.90	567	37.54	-
H19	10 48 25.97	12 32 03.48	267	37.96	-
H20	10 48 25.48	12 32 14.06	642	38.17	16
H21	10 48 25.74	12 32 04.67	404	38.46	17
H22	10 48 26.57	12 31 41.29	165	37.70	-
H23	10 48 25.95	12 31 56.30	416	38.46	18
H24	10 48 25.66	12 32 02.06	490	38.63	19
H25	10 48 26.09	12 31 48.58	331	38.18	-
H26	10 48 25.59	12 31 56.29	724	38.82	20
H27	10 48 24.61	12 32 16.74	468	38.61	22
H28	10 48 25.60	12 31 50.42	549	38.33	21
H29	10 48 24.97	12 32 05.32	331	37.70	-
H30	10 48 25.61	12 31 47.59	452	38.91	-
H31	10 48 24.77	12 32 07.49	423	38.27	23
H32	10 48 24.33	12 32 18.05	198	37.80	-
H33	10 48 24.93	12 32 01.83	704	39.01	24
H34	10 48 23.90	12 32 26.76	495	38.44	-
H35	10 48 24.83	12 31 59.72	504	38.49	-
H36	10 48 24.00	12 32 16.94	457	38.57	26
H37	10 48 24.92	12 31 52.58	239	37.82	-
H38	10 48 23.65	12 32 21.01	358	37.90	-
H39	10 48 25.33	12 31 37.57	463	38.66	27
H40	10 48 25.12	12 31 42.45	396	38.23	28
H41	10 48 24.30	12 32 01.50	880	38.91	29
H42	10 48 23.35	12 32 21.41	564	38.67	31
H43	10 48 23.82	12 32 08.01	1087	39.04	30
H44	10 48 22.92	12 32 24.08	320	38.32	33
H45	10 48 23.32	12 32 11.27	653	38.92	35
H46	10 48 24.49	12 31 40.50	285	38.05	34
H47	10 48 23.69	12 31 56.82	333	37.86	-
H48	10 48 24.32	12 31 39.84	291	38.36	38
H49	10 48 22.45	12 32 23.00	487	38.74	39
H50	10 48 22.17	12 32 19.74	442	38.09	-
H51	10 48 22.47	12 32 11.55	399	38.10	-
H52	10 48 23.03	12 31 57.23	460	38.40	41
H53	10 48 23.13	12 31 51.79	698	39.28	42
H54	10 48 22.62	12 31 58.79	270	37.70	-
H55	10 48 21.73	12 32 16.79	507	38.82	45
H56	10 48 22.63	12 31 53.63	618	38.99	46
H57	10 48 22.38	12 31 59.07	340	38.21	49
H58	10 48 21.52	12 32 19.51	308	38.08	48
H59	10 48 21.70	12 32 09.81	596	38.34	-
H60	10 48 21.52	12 32 12.48	400	38.10	50
H61	10 48 21.31	12 31 59.60	369	38.08	-

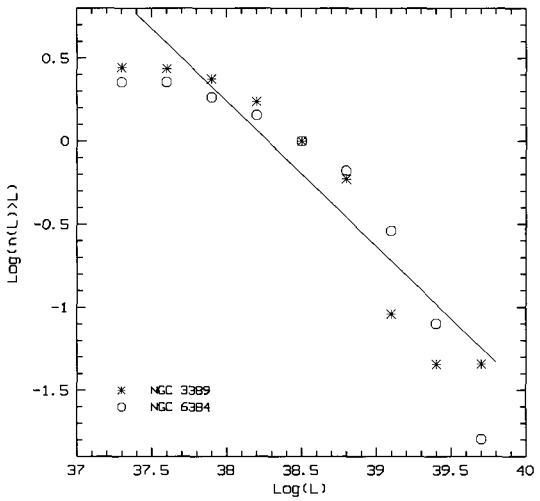

Fig. 4.— The cumulative LF of HII regions on NGC 3389 (stars) in comparsion with that of NGC 6384, (Feinstein 1997) (circles). Solid line is the fitting line for all data points.

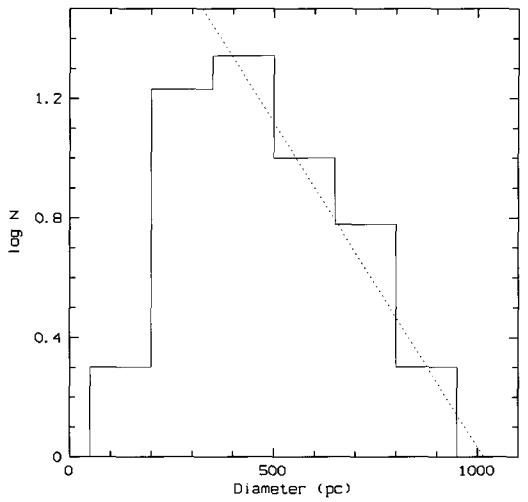

Fig. 5.— Diameter distribution of the HII regions with fitting line (dotted).

The straight line in the Fig. 4 gives the best fit for all data points of NGC 3389 LF, which correspondes to a power law in the form:

$$dN = AL^{\alpha}dL, \quad (2)$$

with a power index α=-1.95±0.24, which is in agreement with α = -2.0±0.2 for Sa-Sb galaxies quoted by Banfi et al. (1993) for a sample of 22 spirals and with α = -2.0±0.5 for a sample of 30 spirals (Kennicutt et al. 1989).

V. Diameter distribution

Fig. 5 shows the diameter distribution for the HII regions of NGC 3389. The number of HII regions with diameter greater than a given diameter value plotted as a function of diameter. The data fit an exponential law, as proposed by the previous works from Van den Berg (1981), Hodge (1983), Hodge (1987) and many others. The exponential law is in the form $N = N_{o}e^{-D/D_{o}}$. We obtain D_{o} = 200 ± 7 pc, which is in agreement with that given by Hodge (1987); 180 pc for NGC 3389, if the smallest diameters were ignored in fitting.

VI. Summary

We have identified 61 HII regions in the spiral galaxy NGC 3389. The positions of fourty of them are identical with those in Hodge & Kennicutt (1983) and 21 are newly identified. The diameters and the fluxes of 61 HII regions of NGC 3389 are measured for the first time. The H_{α} luminosities of HII regions span a range from 3×10^{37} to 6×10^{39} erg s^{-1} as those in most Sa-Sb galaxies. The luminosity function is found to well fit by a power law with an index of -1.95±0.25 which is in agreement with that for early spiral galaxies. In a forthcoming paper, we will discuss the ionization sources of the HII regions and star formation activity in NGC 3389.

ACKNOWLEDGEMENTS

This work is financially supported by SEES-BK21 grant, Korean Government. Abdel-Hamid is very grateful to BK21 and School of Earth and Environmental Science (Astronomy Program) at Seoul National University for their support and good hospitality. We are grateful to P. Hodge for providing us his HII regions data for NGC 3389.

REFERENCES

Banfi, R., Chincarini, G., & Henry, R. B. C. 1993, HII regions in spiral galaxies: positions, luminosity function and diameter distribution, A&A, 280, 373

Bell, E., & Kennicutt, R. C., Jr. 2001, A comparison of ultraviolet imaging telescope far-ultraviolet and H_{α} star formation rates, ApJ, 548, 693

de Vaucouleurs, G., de Vaucouleurs, A., Corwin, H. G.Jr., Buta, R. J., Paturel, G., & Fouque, P. 1991, The 3rd Reference Catalog of Bright Galaxies, Spring-Verlag, New York.

Feinstein, C. 1997, HII regions in southern spiral galaxies: The H_{α} luminosity function, ApJS, 112, 29

Hodge, P. W. 1983, Size distributions of H II regions in galaxies. I - Irregular galaxies, AJ, 88, 1323

Hodge, P. W. 1987, Size distribution of HII regions in galaxies: II. Spiral galaxies, PASP, 99, 915

Hodge, P. W., & Kennicutt, R. C., Jr. 1983, An atlas of HII regions in 25 galaxies, AJ, 88, 296

Hodge, P. W., Lee, M. G., & Kennicutt, R. C., Jr. 1989, The HII regions of NGC 6822. II. The luminosity function and size distribution, PASP, 101, 32

Kennicutt, R. C., Jr., Edgar, B. K., & Hodge, P. W. 1989, Properties of HII region populations in galaxies. II. The HII region luminosity function, ApJ, 337, 761

Kennicutt, R. C., Jr., & Kent, S. M. 1983, A survey of H-alpha emission in normal galaxies, AJ, 88, 109

Kennicutt, R. C., Jr. 1983, The rate of star formation in normal disk galaxies, ApJ, 272, 54

Sandage, A., & Tamman, G. 1981, A revised Shapley-Ames Catalog of Bright Galaxies (Washington:Carneige Institution of Washington).

Schlegel, D. J., Finkbeiner, D. P. & Davis M. 1998, Maps of Dust Infrared Emission for Use in Estimation of Reddening and Cosmic Microwave Background Radiation Foregrounds, ApJ, 500, 525.

Shanks, T. 1997, A test of Tully-Fisher distance estimates using Cepheids and SNIa, MNRAS, 290, L77.

Thilker, D. A., Walterbos R. A. M., Braun R., & Hoopes C. G. 2002, HII regions and Diffuse ionized Gas in 11 nearby spiral galaxies, ApJ, 124, 3134.

Tully, R. B. 1988, Nearby Galaxies Catalog (Cambridge University Press).

van den Berg, S. 1981, Frequency Distribution of HII region Diameters, AJ, 86, 1464.